Supplementary Information

Reciprocal coupling of coagulation and innate immunity via neutrophil serine proteases.

Steffen Massberg, Lenka Grahl, Marie-Luise von Bruehl, Davit Manukyan, Susanne Pfeiler, Christian Goosmann, Volker Brinkmann, Michael Lorenz, Kiril Bidzhekov, Avinash Khandagale, Ildiko Konrad, Elisabeth Kennerknecht, Katja Reges, Stefan Holdenrieder, Siegmund Braun, Christoph Reinhardt, Michael Spannagl, Klaus T. Preissner and Bernd Engelmann
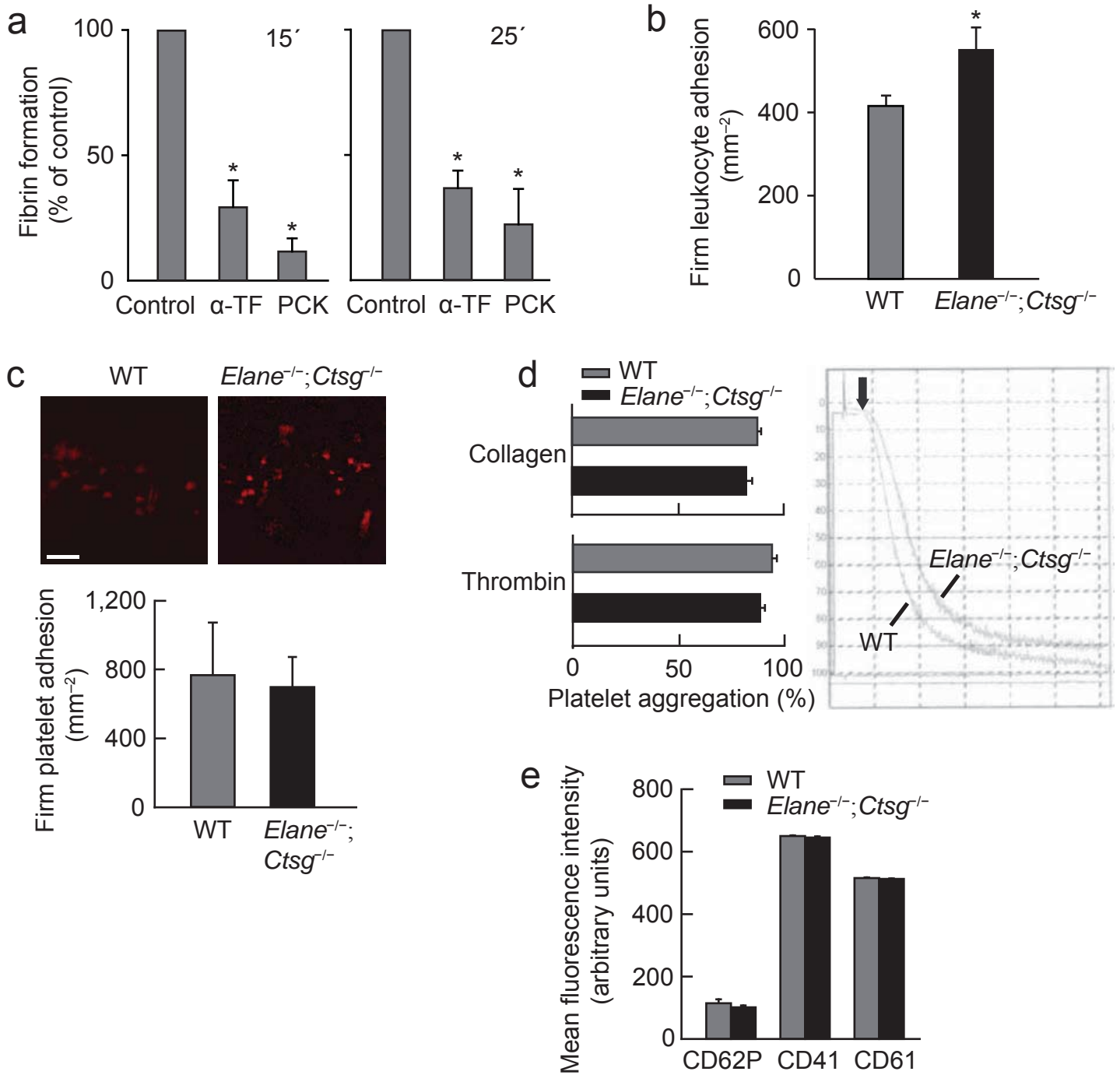
Contents:

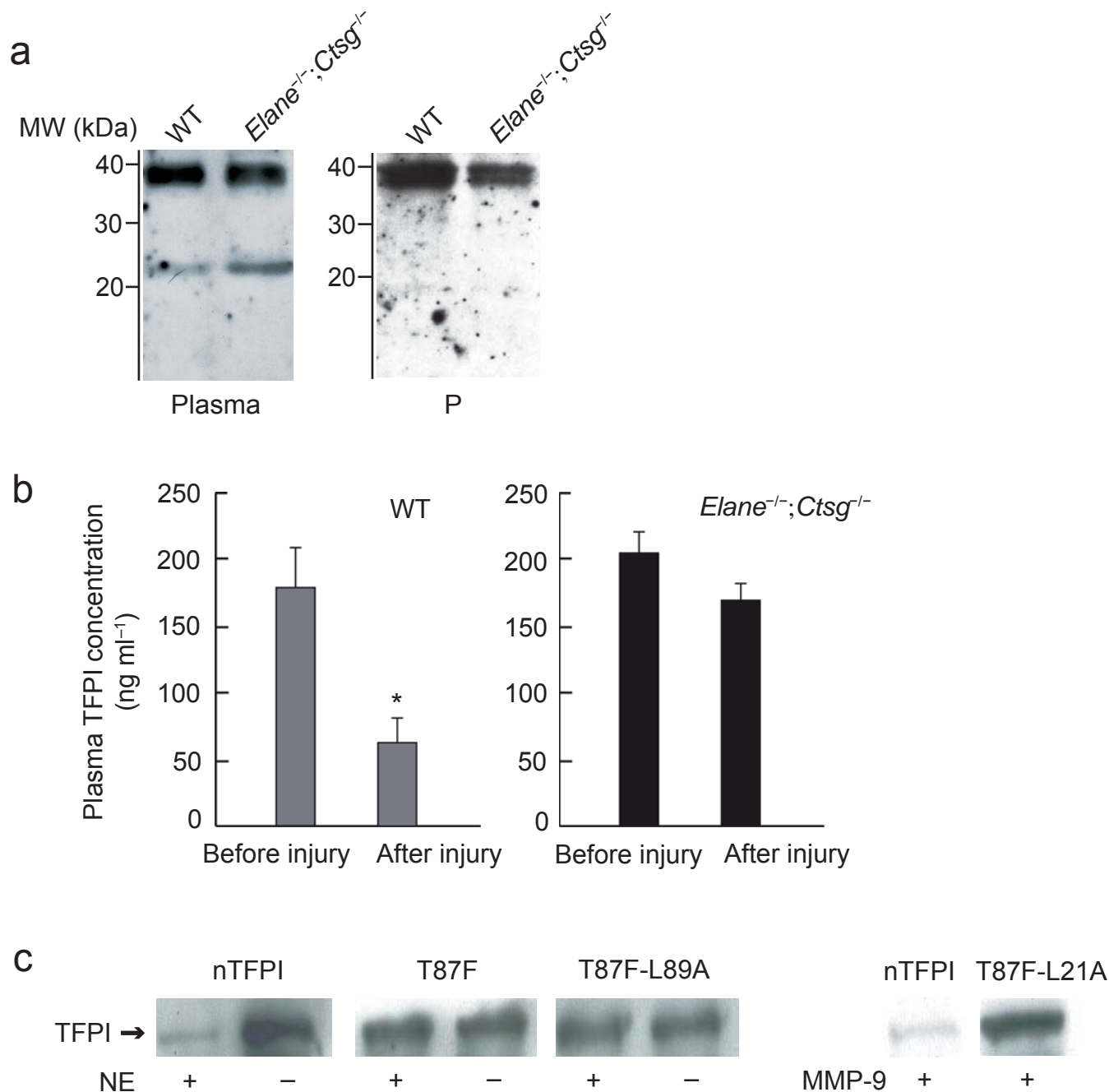**Supplementary Figure 1. Blood cell adhesion and activation in neutrophil serine protease-deficient mice in vivo.** (**a**) Triggers of *in vivo* coagulation after FeCl$_3$-induced vessel injury. Antibody to mouse tissue factor (10 µg g^{-1} weight) and factor XII inhibitor PCK (8 µg g^{-1} weight) were infused into WT mice before vessel injury. Values refer to time interval after the end of injury period. Controls (isotype IgG) set as 100%. n = 4 mice per group, *$P < 0.05$. (**b**) Adhesion of acridine orange-labeled leukocytes to the carotid lesion. 10 min after ligation injury of carotid artery. Leukocytes were of the same genotype as the recipient mice. n = 4–6 per group, *$P < 0.05$. (**c**) Firm adhesion of rhodamine 6G-labeled platelets to the disrupted vessel wall (10 min after ligation injury). Platelets were of the same genotype as the recipient mice. Top: Representative images. Bottom: Quantitative measurements. n = 3 per group. Bar, 10 µm. (**d**) Platelet activation in *Elane$^{-/-}$;Ctsg$^{-/-}$* mice. Platelets recovered from WT and *Elane$^{-/-}$;Ctsg$^{-/-}$* animals were stimulated with collagen (10 µg ml^{-1}) or thrombin (1 U ml^{-1}) and the kinetics of activation monitored by aggregometry. Left: Mean values of n = 2–3 experiments per group. Right: Representative aggregometer profiles. (**e**) Platelet adhesion receptor levels in *Elane$^{-/-}$;Ctsg$^{-/-}$* mice. Platelets from WT and *Elane$^{-/-}$;Ctsg$^{-/-}$* animals were activated with thrombin and subsequently analyzed for surface exposure of the indicated adhesion molecules by flow cytometry. CD62P, P-selectin; CD41, integrin αIIb; CD61, integrin β3.
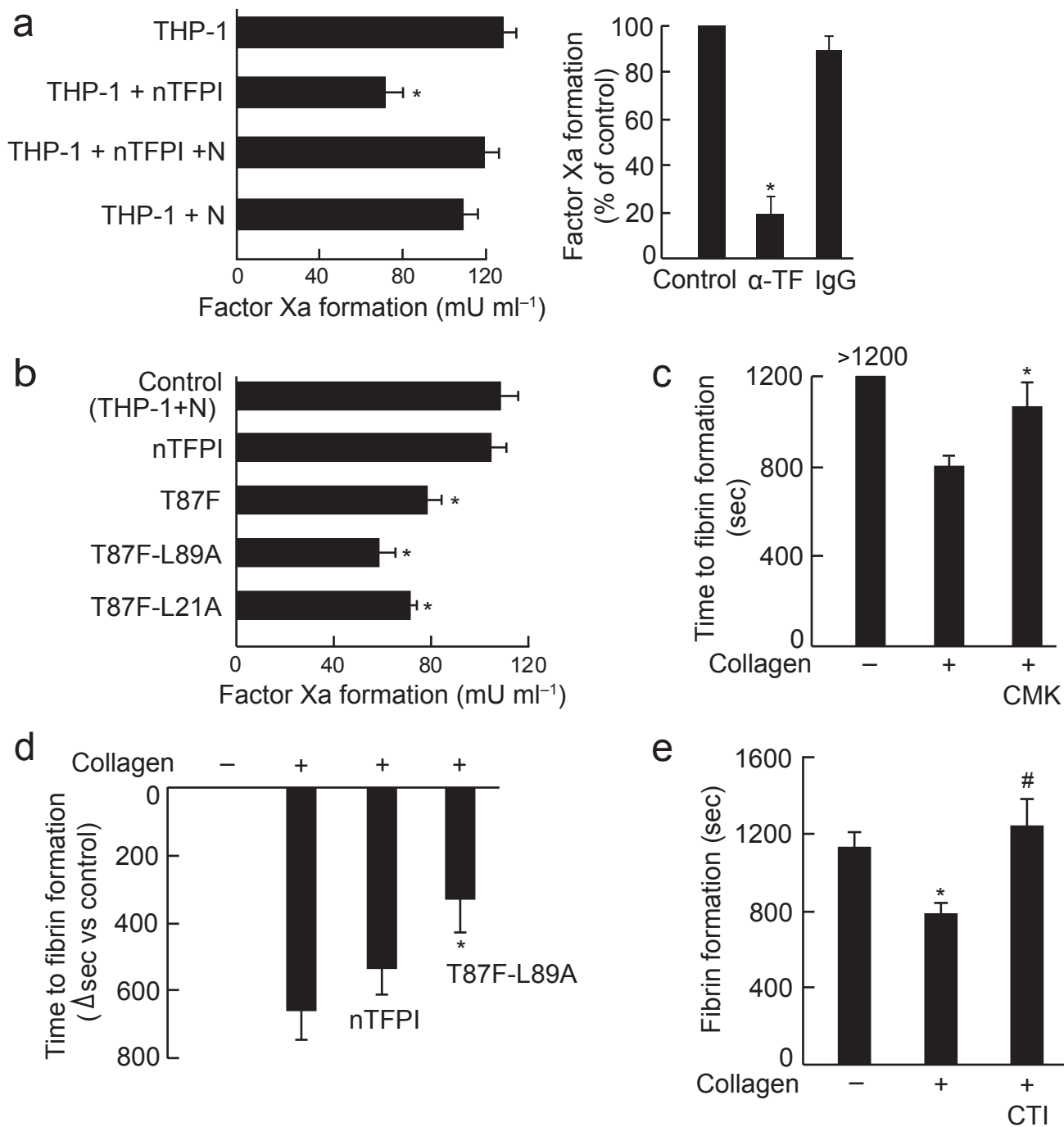
Supplementary Figure 2

a

b

c
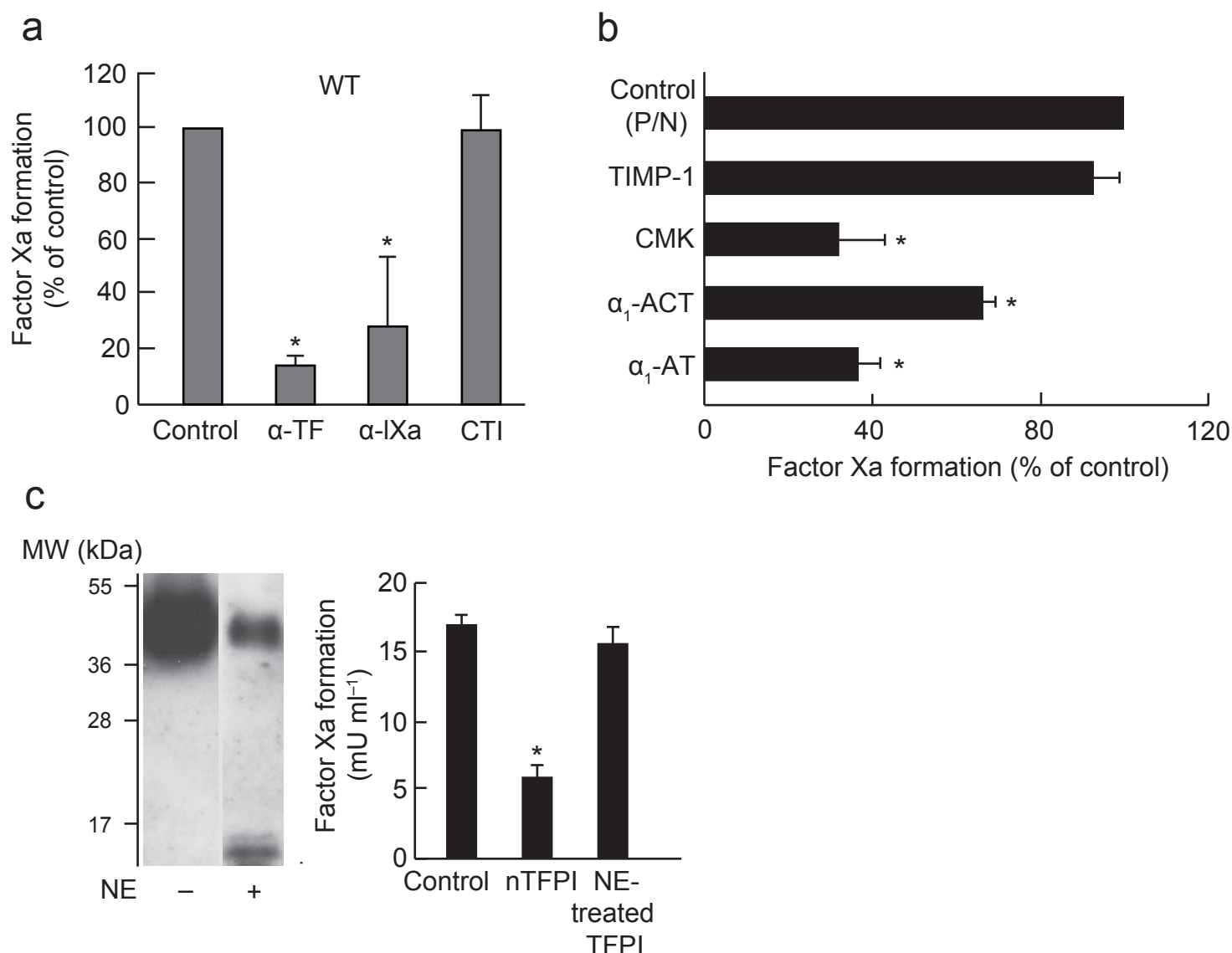
Supplementary Figure 2. Functional implications of TFPI degradation by neutrophil serine proteases. (**a**) Triggers of procoagulant activity in mixtures of neutrophils (N) and activated platelets (P). Procoagulant activity in suspensions of mouse neutrophils and platelets (both WT) was measured using coagulation factor concentrate. Antibodies to tissue factor and FIXa were used at 50 μg ml^{-1} and 30 μg ml^{-1}, respectively. CTI, 5 μg ml^{-1}. 100% represents respective control value (isotype IgG in case of antibodies or vehicle in case of CTI). n = 4 per group, *$P < 0.05$ (versus control). (**b**) Inhibitors of neutrophil serine proteases decrease procoagulant activity *in vitro*. Human neutrophils (10^7) and platelets (10^8) were coincubated for 15–20 min in the presence of collagen (8 μg ml^{-1}). Determination of procoagulant activity by coagulation factor concentrate. The following protease inhibitors were used: TIMP-1 (0.1 μg ml^{-1}), CMK (0.5 mM), alpha-1-antichymotrypsin (10 μg ml^{-1}), alpha-1-antitrypsin (10 μg ml^{-1}). n = 3–5 per group, *$P < 0.05$ (versus control). (**c**) Loss of anticoagulant activity after TFPI cleavage induced by neutrophil elastase (NE). Left: nTFPI (0.5 μg) is degraded after incubation with neutrophil elastase (5 ng, 30 min). Western blots with antibody to TFPI Kunitz-1 domain. Right: Neutrophil elastase-pretreated TFPI fails to inhibit the procoagulant activity induced by THP-1 cells. n = 4 per group, *$P < 0.05$.

Supplementary Figure 3. Degradation and thrombus recruitment of TFPI. (**a**) Plasma and platelet TFPI after vessel injury. Western blots of TFPI in plasma and platelets (P) recovered from WT and $Elane^{-/-};Ctsg^{-/-}$ mice 15 min after $FeCl_3$-induced carotid injury. The enhanced density of the TFPI degradation product in plasma of $Elane^{-/-}; Ctsg^{-/-}$ mice could suggest that this cleavage product is subject to further degradation by neutrophil serine proteases. (**b**) Plasma TFPI concentrations before and after vessel injury. Bilateral damage of carotid arteries was induced by exposure to $FeCl_3$. WT: n = 8 (before injury; in 4 of these mice measurements were only performed before injury), n = 4 (after injury). $Elane^{-/-};Ctsg^{-/-}$: n = 3 (before and after injury). *$P < 0.05$. (**c**) Resistance of TFPI mutants to degradation by serine proteases. nTFPI and TFPI variants with mutations at the cleavage sites for serine proteases (T87F, L89A) and for matrix metalloproteases (L21A) were incubated for 30 min with isolated neutrophil elastase (10 nM) or MMP-9 (200 nM) and TFPI degradation was analyzed by western blotting. Under the same conditions, cathepsin G (50 nM) induced degradation of nTFPI, but not of the T87F-L89A variant (not shown).
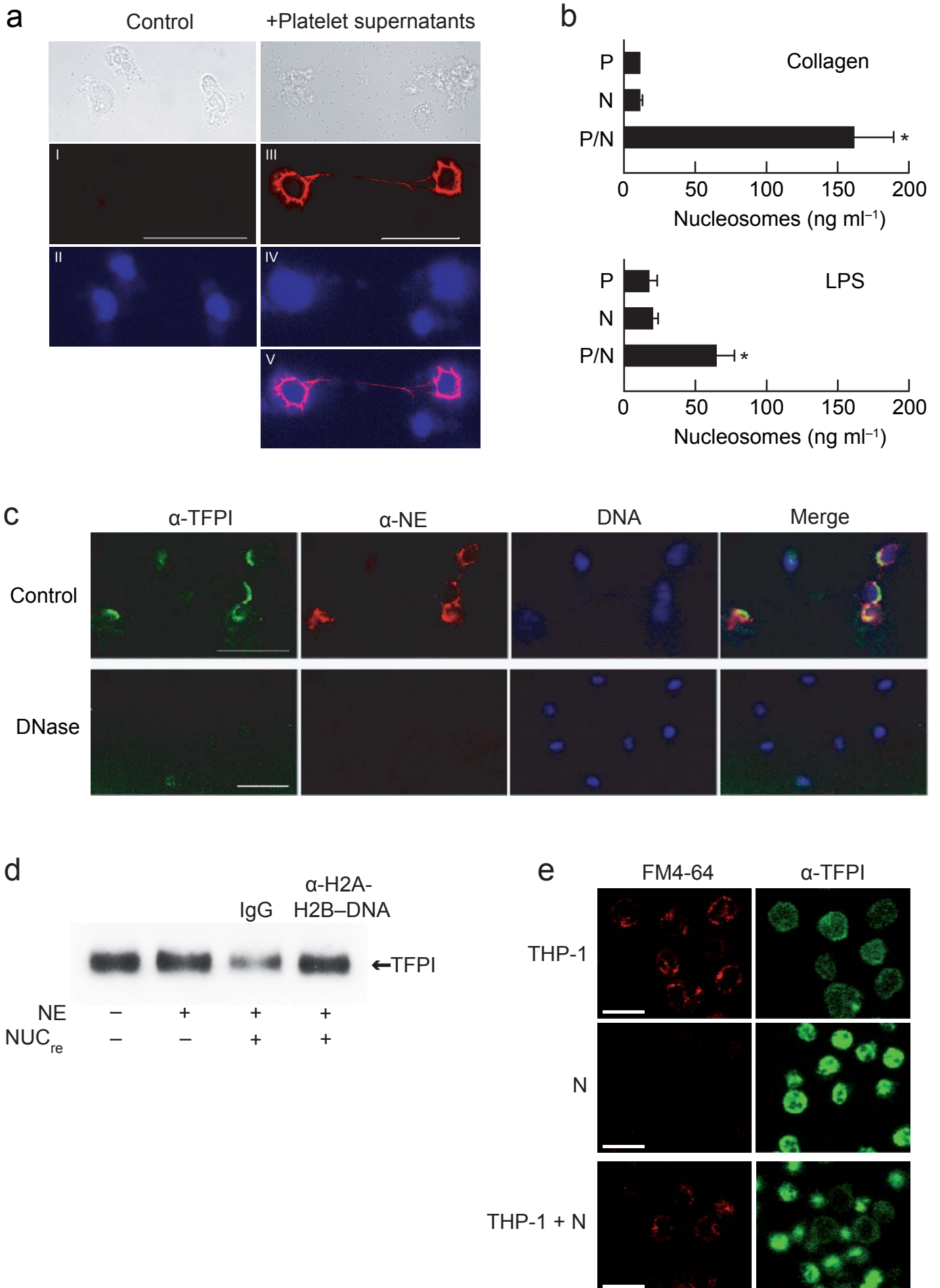
Supplementary Figure 4. Effect of TFPI mutants on tissue factor-induced procoagulant activity in vitro. (**a**) Effect of neutrophils on inhibition of procoagulant activity by TFPI. Left: Inhibition of the procoagulant activity of THP-1 cells (10^5) by nTFPI (0.5 nM) is reverted by human neutrophils (10^4). Right: Procoagulant activity of THP-1 cells is suppressed by tissue factor-specific antibody (10 μg ml^{-1}). n = 3 per group, *$P < 0.05$ (versus THP-1 alone (left) or versus control (right)). (**b**) Effect of TFPI mutants on procoagulant activity of THP-1 cells in the presence of neutrophils. Experiments performed under the same conditions as in (**a**) but in the presence of nTFPI or TFPI mutants (all at 0.5 nM). n = 3–13 per group, *$P < 0.05$ (versus control). (**c**) Whole blood coagulation requires neutrophil elastase. To whole human blood activated with collagen CMK (0.5 mM) was added. Time interval until fibrin formation was measured by thrombelastography. n = 3–4 per group, *$P < 0.05$ (versus same situation without CMK). (**d**) Effect of T87F-L89A variant on fibrin generation *ex vivo*. nTFPI or T87F-L89A (0.5 nM) were added to collagen-activated human whole blood. Values refer to difference versus fibrin formation without collagen. n = 4 per group, *$P < 0.05$ (versus collagen alone). (**e**) Factor XII inhibition blocks whole blood fibrin formation. We added the factor XIIa inhibitor CTI (50 μg ml^{-1}) to human whole blood activated with collagen (8 μg ml^{-1}). Fibrin formation was determined by thrombelastography. n = 3–5 per group, *$P < 0.05$ versus without collagen, #$P < 0.05$ versus collagen alone.

Supplementary Figure 5
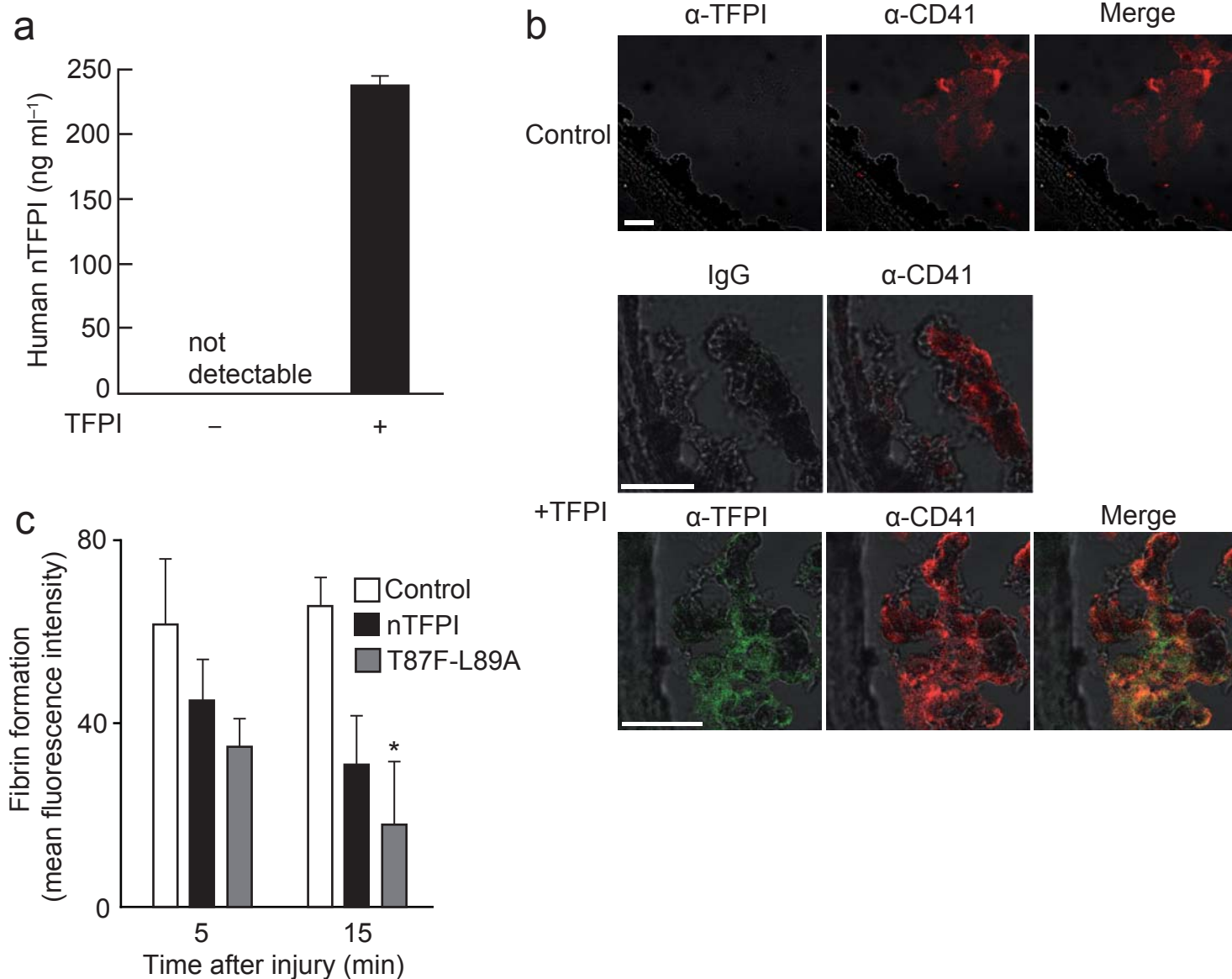
Supplementary Figure 5. Effects of TFPI infusion in vivo. (**a**) Plasma concentration of human TFPI in mice. nTFPI (3 μg) was injected into WT mice. Plasma concentration of human TFPI was measured by Elisa specifically detecting human TFPI. The median value for mouse TFPI in plasma was 189 ng ml^{-1}. n = 4 mice per group. (**b**) Recruitment of TFPI to thrombi. After injection of human nTFPI, carotid vessels of mice were injured (FeCl$_3$), the thrombi were excised and analyzed for the presence of TFPI using an Alexa488-labeled antibody to human TFPI (green) or respective control antibody (both labeled with Alexa488). Thrombus-associated platelets were visualized with CD41-specific antibody (red). Upper row, no TFPI injection; middle row, injection of TFPI, presence of isotype-matched control antibody; bottom row, injection of TFPI, TFPI-specific antibody. Bars, 20 μm. (**c**) Effect of nTFPI versus TFPI mutant on fibrin deposition during large vessel thrombosis. nTFPI or T87F-L89A mutant were injected before FeCl$_3$-induced injury. Then fibrin deposition at the injury site was measured by intravital microscopy. Values refer to time periods after injury. n = 4 per group, *$P < 0.05$ versus control.

Supplementary Figure 6

a

Control   +Platelet supernatants

b

Collagen

LPS

c

α-TFPI   α-NE   DNA   Merge

Control

DNase

d

IgG   α-H2A-H2B–DNA

←TFPI

NE   −   +   +   +

NUC$_{re}$ −   −   +   +

e

FM4-64   α-TFPI

THP-1

N

THP-1 + N
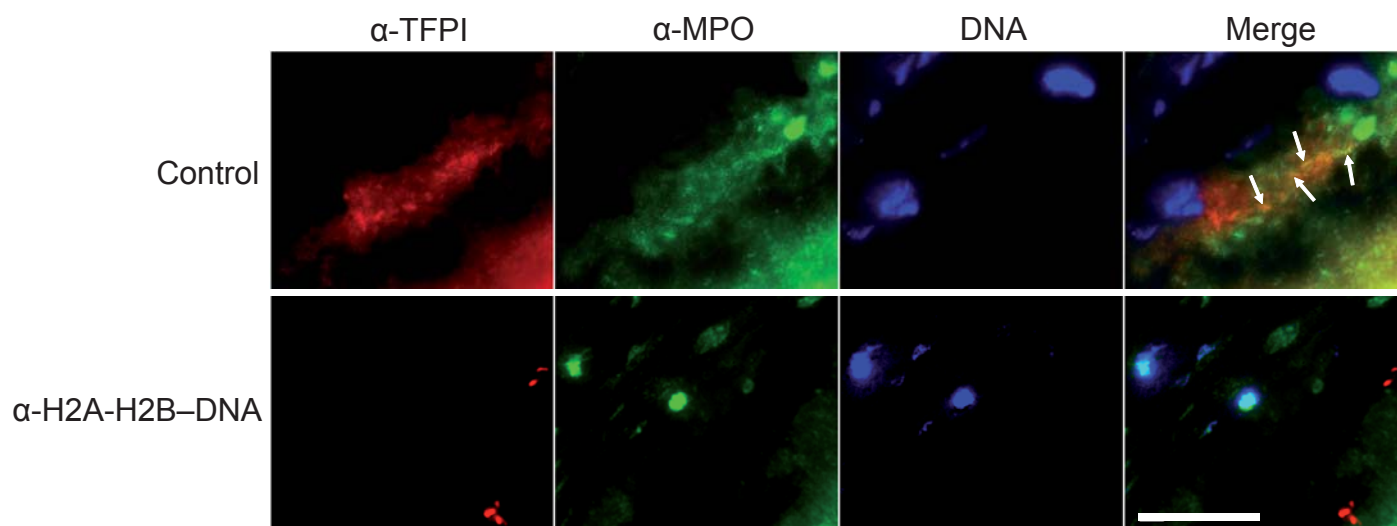
Supplementary Figure 6. Release of nucleosomes from neutrophils in vitro. (**a**) Visualization of nucleosome release from neutrophils. Isolated human neutrophils (ficoll method; activated with PMA, 100 nM) were incubated for 15 min without (I–II) or with (III–V) supernatants recovered from collagen-activated platelets. Representative confocal microscopy images of externalized nucleosomes (I, III; recognized by H2A-H2B–DNA–specific antibody (red)). II, IV: DNA stained with Hoechst 33342 (blue). V: Costaining of both fluorophores. Bars, 50 µm. (**b**) Quantitative determination of nucleosome release from neutrophils. Neutrophils (N; ficoll method) preactivated with PMA (100 nM) were coincubated with platelets (P) for 15–20 min in presence of collagen (8 µg ml^{-1}; upper panel) or for 30 min with lipopolysaccharide (LPS, 5 µg ml^{-1}; lower panel). We used Elisa to quantify nucleosomes in the supernatants recovered from the blood cell suspensions. n = 4–10 per group, *P < 0.05 (versus P or N). (**c**) Co-assembly of neutrophil elastase and TFPI on neutrophil surface. Preactivated neutrophils were coincubated with supernatants recovered from collagen-activated human platelets without or with DNase. TFPI (green), neutrophil elastase (red), DNA (blue). Bar, 50 µm. (**d**) Effect of antibody to H2A-H2B–DNA on nucleosome-induced TFPI proteolysis. Degradation of TFPI (0.5 µg) by neutrophil elastase (7 ng) without or with NUC$_{re}$ (1 ng ml^{-1}) was analyzed by western blotting in the presence of H2A-H2B–DNA–specific antibody or isotype-matched control antibody (10 µg ml^{-1}). (**e**) Effect of neutrophils on TFPI binding to cell surface of THP-1 cells. Weak binding of TFPI (green) to THP-1 cells (10^5) is further lowered after a 30 min incubation of the cells with neutrophils (10^5, previously stimulated with PMA plus supernatants recovered from activated human platelets). FM4-64 (red), labeling of cell membrane of THP-1 cells. Bar, 20 µm.
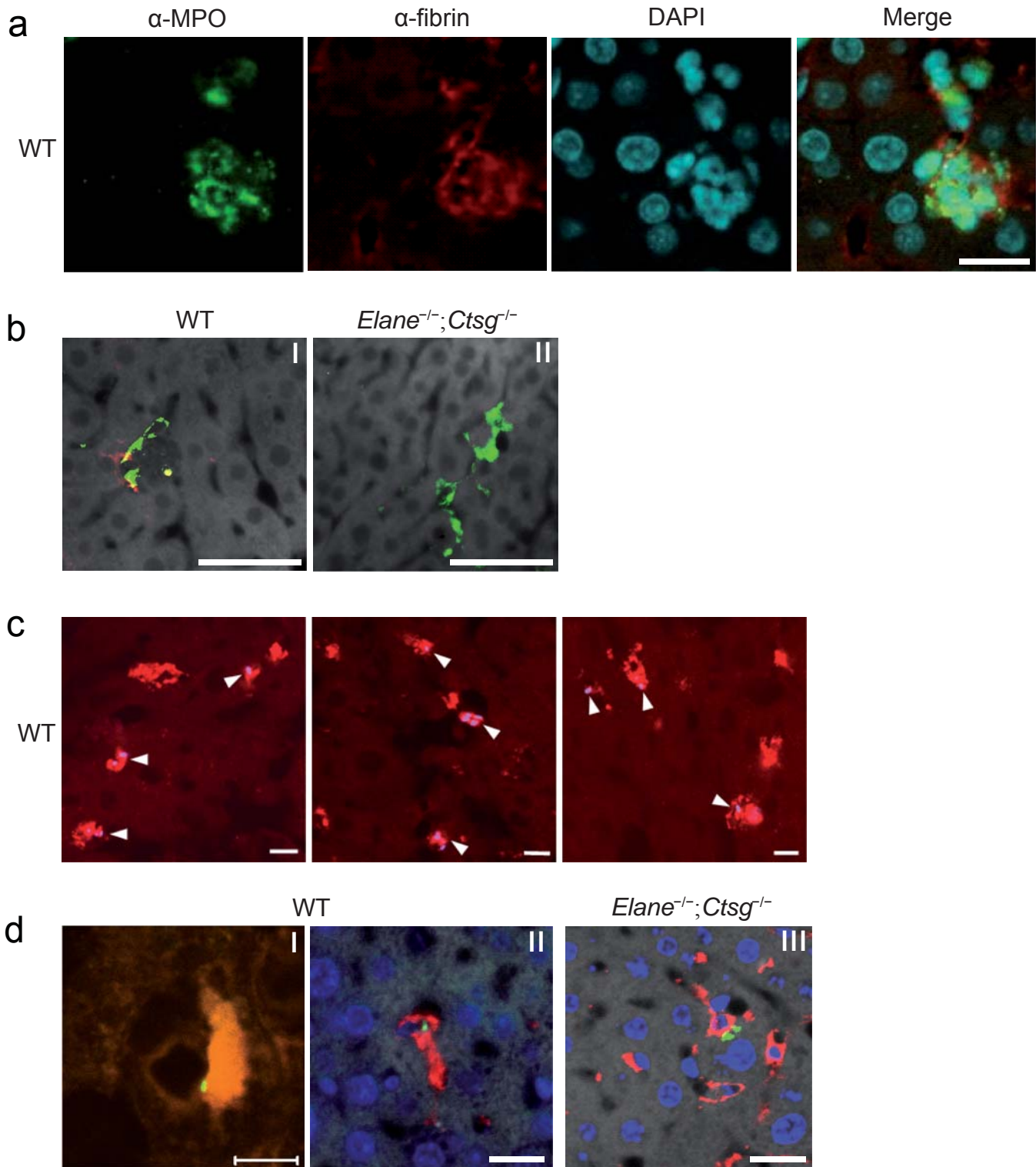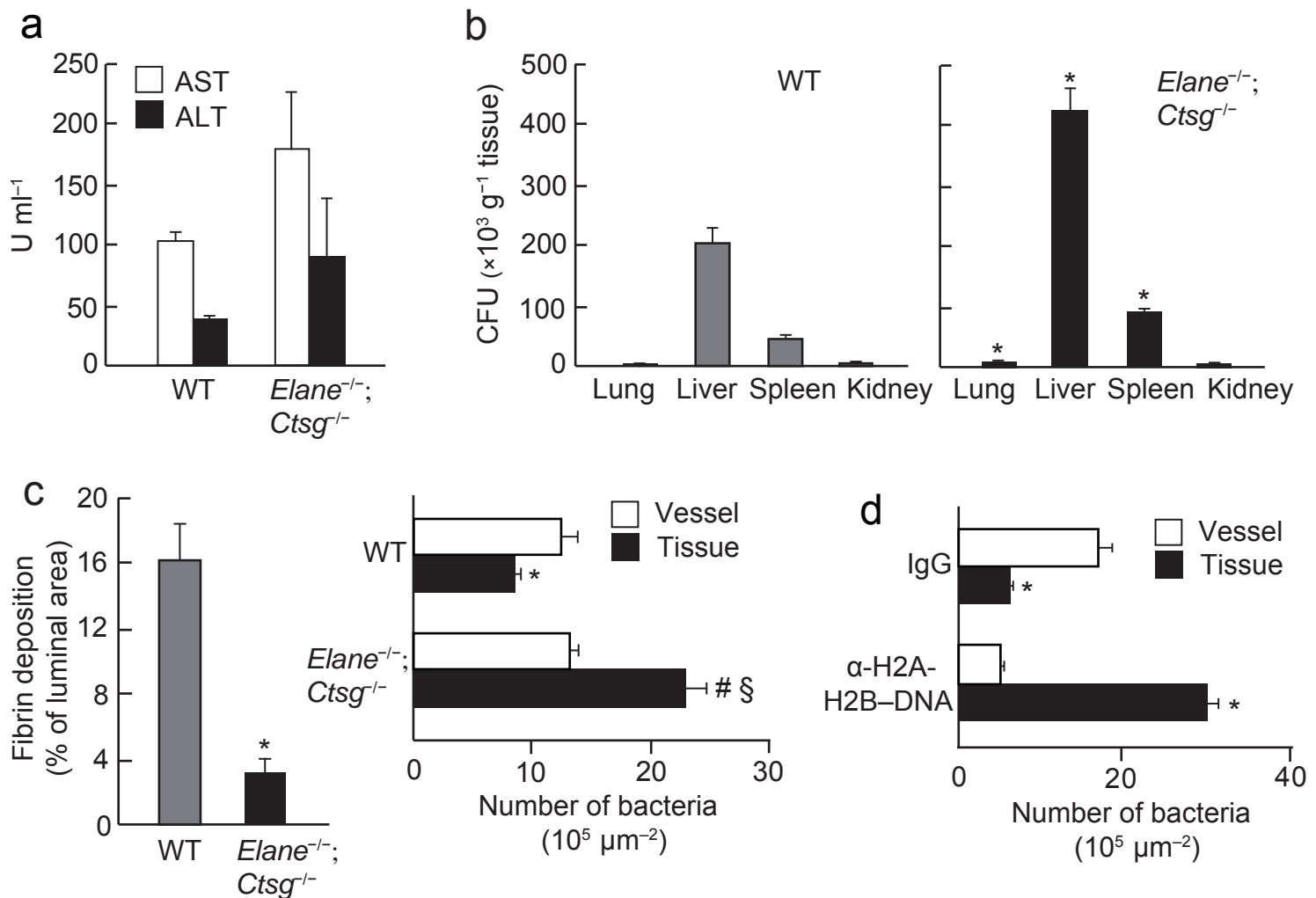
Supplementary Figure 7

Supplementary Figure 7. Effect of nucleosomes on TFPI binding to thrombi in vivo. Injection of antibody to H2A-H2B–DNA (or control IgG) into WT mice. FeCl$_3$ model, 30 min. TFPI (red), myeloperoxidase (MPO, green; used to identify neutrophils), DNA (blue). Pseudocolor images. Arrows indicate colocalization of TFPI with MPO. Bar, 25 μm.

Supplementary Figure 8

Supplementary Figure 8. Fibrin association with neutrophils and Kupffer cells during systemic infection. (a) Fibrin colocalizes with neutrophils in liver microvessels. 6 h after systemic infection with *E. coli*, fibrin (visualized with labeled fibrin-specific antibody; red) accumulates in the vicinity of activated neutrophils (detected with labeled MPO-specific antibody; green) in liver microvessels of WT mice. Cell nuclei (blue). Bar, 15 μm. (b) Association of fibrin with Kupffer cells. Intravascular fibrin (labeled fibrin-specific antibody; red) partially colocalizes with Kupffer cells (labeled F4-80-specific antibody; green) in liver microvessels of WT mice but to a lesser extent in neutrophil serine protease-deficient animals. Pictures obtained with Multispectral Imaging system. Bar, 50 μm. (c) Colocalization of fibrin and *E. coli*. GFP-*E. coli* (blue, pseudocolored) and fibrin (red) in WT livers (indicated by arrow heads). Bars, 10 μm. (d) Association of *E. coli* with Kupffer cells. GFP-labeled bacteria (green) are associated with Kupffer cells (red) in the hepatic microcirculation during systemic infection. Pictures obtained with Multispectral Imaging system. Bars: I, 5 μm; II–III, 20 μm.
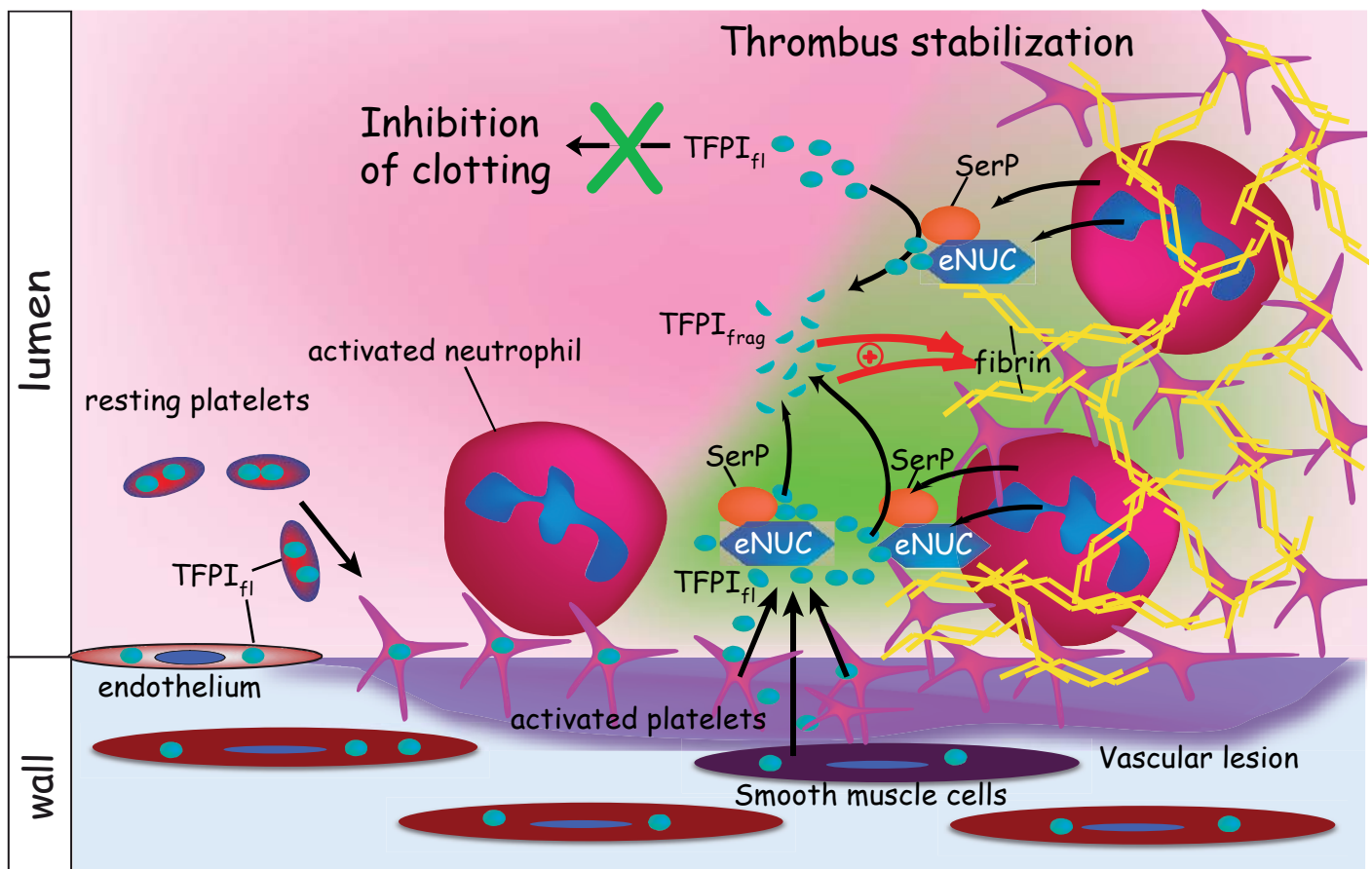
Supplementary Figure 9

Supplementary Figure 9. Parameters of liver damage and organ distribution of bacteria.
(**a**) Liver damage parameters in WT and neutrophil serine protease-deficient animals. Aspartate
aminotransferase (AST) and alanine aminotransferase (ALT) were determined in plasma from *E. coli*
infected WT and *Elane*$^{-/-}$;*Ctsg*$^{-/-}$ mice 6 h after start of infection. n = 4 mice per group. (**b**) Bacterial
counts in organs of WT and *Elane*$^{-/-}$;*Ctsg*$^{-/-}$ mice after infection with *E. coli*. CFUs in the indicated
organs were determined 6 h after infection. n = 4 per group, *$P < 0.05$ (versus same organ in WT
mice). (**c**) Fibrin deposition and bacterial distribution in microvessels of spleen. Fibrin-positive area
(visualized with Alexa594-labeled fibrin-specific antibody) and distribution of *GFP-E. coli* in splenic
microcirculation. Splenic sinusoids were identified by stabilin-2-specific antibody. > 950 vessels per
group. n = 3 per group, *$P < 0.05$ versus vessel in WT, [#]$P < 0.05$ versus tissue in WT, [§]$P < 0.05$ versus
vessel in *Elane*$^{-/-}$;*Ctsg*$^{-/-}$. (**d**) H2A-H2B–DNA–specific antibody increases tissue invasion of bacteria.
Localization of *GFP-E. coli* in the hepatic microcirculation of WT mice after systemic infection. >
1,500 vessels per group. n = 4 per group, *$P < 0.05$ (versus vessel).

Supplementary Figure 10. Model of intraluminal coagulation induced by the concerted action of neutrophil serine proteases and extracellular nucleosomes. Blood neutrophils that are recruited to vessel lesions or interact with bacteria in microvessels are activated and release nucleosomes, a process supported by surrounding activated platelets. Additionally, nucleosomes might also be liberated from damaged vessel wall cells. The externalized nucleosomes capture endogenous anticoagulants such as TFPI which is released from activated platelets and disrupted vessel wall cells or is directly recruited from plasma. This enables extracellular neutrophil serine proteases to proteolytically inactivate TFPI. Hence the inhibitory effect of TFPI on coagulation is reverted and fibrin formation is increased, which in turn stabilizes thrombus development. As a consequence, bleeding from vessel injuries is diminished. Aside from this, vessel occlusions are promoted which restrict tissue invasion of bacteria in the microcirculation, but also favor thrombosis in large vessels. $TFPI_{fl}$, full-length TFPI; $TFPI_{frag}$, TFPI fragments; eNUC, extracellular nucleosomes; SerP, neutrophil serine proteases.

Supplementary methods

Cells. We prepared human neutrophils by incubation of freshly prepared buffy coats with microbeads coupled to CD15-specific antibodies (microbead isolation; Miltenyi Biotec) for 15 min at 8°C[1]. Then the suspensions were applied to the positive selection column and neutrophils were eluted from the column by PBS containing additionally bovine serum albumin (0.5%) and EDTA (0.18%). In some experiments (ficoll isolation), we isolated neutrophils by first adding dextran (3%; MW 500,000) to whole blood (1:2) and allowing red blood cells to separate for 30 min. The supernatant was then removed and layered on top of ficoll (1:1) and centrifuged for 30 min (240 x g). The pellet was suspended in HBSS buffer and layered on a gradient of histopaque 1119 and histopaque 1077 (1:1). After 30 min of centrifugation, we recovered the neutrophils from the border area between the two different types of histopaque. In other experiments, we subjected the pellet to hypotonic lysis for 1 min (pyrogen-free H_2O), centrifuged the suspensions and recovered the pellet. Thereby, comparable results were obtained with neutrophils isolated by using the histopaque gradient. The suspensions obtained with the microbead and ficoll isolation procedures contained > 95% of neutrophils in all cases. For isolation of mouse neutrophils, femur and tibia were recovered from both WT and *Elane*^{−/−};*Ctsg*^{−/−} mice and the distal parts of the bones were cut off. The bone marrow was extruded by rinsing with HBSS-EDTA plus BSA (1%). We centrifuged the cell suspensions (400 g, 10 min, 4°C) and resuspended them in HBSS-EDTA. Subsequently the cells were positioned on a three-layer Percoll gradient of 78%, 69%, and 52% Percoll (Amersham Pharmacia Biotech), respectively, as described before[2]. The neutrophils from the 69%/78% interface and the upper part of the 78% layer were collected in tubes coated with BSA (1%). The cells were washed once, residual red blood cells were eliminated by hypotonic lysis, and the neutrophils (purity of 90%) were suspended in the appropriate buffers.

TFPI variants. We amplified the full-length human TFPI (isoform TFPIα) gene from carotid artery cDNA, using the forward outer primer 5'-GTACATGCACTTTGGGCTTC-3' and the reverse outer primer 5'-TCACATATCTTTAACAAGAATTC-3'. After cloning into the expression vector pASK-IBA3 (IBA), we performed site directed mutagenesis with the GENE Taylor kit (Invitrogen), yielding the T87F, T87F-L89A and T87F-L21A variants. LB[amp] medium was inoculated with BL21 *E. coli* and anhydrotetracycline (IBA, 200 ng ml^{−1}) was included into the medium to induce the expression of nTFPI and of TFPI variants. Sequencing verified the correct structure of the variants. The supernatant from the bacterial lysate was collected, passed over a Strep-Tactin II column, and TFPI was purified from the eluate.

Immunofluorescence of ex vivo thrombi. We excised thrombus-containing vessel sections 30 min after carotid injury (FeCl$_3$), fixed them in 1% PFA/PBS and embedded them in paraffin. 5 μm sections were rehydrated, subjected to antigen retrieval (Labsolution, Polysciences Inc), blocked (PBS containing 5% goat serum and 0.05% Tween 20) and reacted with primary antibodies at 37°C overnight in a moist chamber. TFPI was visualized with goat antibody to mouse TFPI (Santa Cruz) detected with Cy3-labeled donkey antibody to goat IgG (Jackson Immuno). MPO-specific antibody (DAKO) was visualized with (secondary) donkey antibody to rabbit IgG coupled to Cy5 (Jackson Immuno). DNA was visualized with BisBenzimide 33342 (Hoechst 33342). The antibody directed to the subnucleosomal complex composed of H2A, H2B and DNA (used to detect externalized nucleosomes) only faintly stains the periphery of nuclei in resting neutrophils, whereas in cells with externalized nucleosomes, the area stained by the antibody and by DNA markers is markedly enlarged and more homogenously distributed[3]. The stained sections were mounted with Mowiol (Calbiochem). We analyzed the specimens with a confocal microscope (SP5, Leica).

Platelet aggregation and flow cytometry. We isolated mouse platelets from blood obtained from the left ventricle (anticoagulated with lepirudin (50 mg ml^{-1}, 1:10). Platelets were stimulated with either collagen (10 μg ml^{-1}) or thrombin (1 U ml^{-1}) and platelet aggregation was monitored by optical aggregometry using a two-channel Chronolog aggregometer (Nobis). For flow cytometry, the surface expressions of platelet cell membrane proteins were determined in isolated mouse platelets (activated with thrombin, 0.5 U ml^{-1}) using PE- or FITC-labeled CD62P-, CD41- and CD61-specific antibodies as described previously[4].

Confocal microscopy in vitro. To prepare platelet supernatants, we activated isolated human platelets (10^9) with 8 μg ml^{-1} collagen (type I, Nycomed) and 0.1 U ml^{-1} thrombin for 30 min at 37°C. After centrifugation, we collected the supernatant. Then, we plated freshly isolated human neutrophils (ficoll isolation) on poly-L-lysine coated FluoroDishes and incubated them for 15 min at 37°C with the platelet supernatants in the presence of aprotinin (20 μg ml^{-1}) plus PMA (100 nM). In some cases, during this incubation, the neutrophils were treated with DNase I (10 U ml^{-1}; Sigma), washed, and resuspended with platelet supernatants (containing TFPI). In other cases, instead of activation by collagen and thrombin, platelets were activated for 30 min with LPS (5 μg ml^{-1}, 37°C). Subsequently, they were incubated for another 15 min in the presence of neutrophils and LPS (37°C). In some experiments, THP-1 cells (FM4-64 labeled) were incubated with activated neutrophils for 15 min in the presence of TFPI (5 nM).

Then unbound TFPI was washed away with PBS. Thereafter, the cells were fixed in all cases with 4% PFA in PBS. They were then washed three times with PBS and then incubated with blocking buffer (5% fish gelatine, 5% donkey serum, 1% BSA, 0.05% Tween 20 in PBS (pH 7.4)) for 30 min at 37°C. Subsequently, the samples were stained with antibody to human neutrophil elastase (10 µg ml^{-1}, Santa Cruz) for 30 min, and, after washing, with secondary Cy3-labeled antibody (Jackson Immuno). To detect TFPI, we stained cells with an Alexa488-labeled human TFPI-specific antibody (10 µg ml^{-1}, Santa Cruz). Cells were also washed three times with PBS and twice with H$_2$O before incubation with BisBenzimide 33342 (Hoechst 33342) to detect DNA. Neutrophils isolated using microbeads exhibited similar colocalization of TFPI with externalized nucleosomes and NE on their surface as neutrophils prepared with the ficoll method. Visualization was performed by confocal microscopy using a Zeiss LSM 510 META, based on an inverted Axiovert 200 MOT microscope. A 63x magnification was obtained with the use of Plan-Apochromat lenses (numerical aperture 1.4, oil immersion). Image acquisition was performed using Zeiss LSM Browser software, and for the image processing Adobe Photoshop was employed.

Western blots. To determine TFPI degradation in mouse thrombi *in vivo*, thrombi adherent to injured carotid artery sections (FeCl$_3$) were excised and analyzed for TFPI and its degradation products by western blotting. Usually, 30 min after induction of injury the common carotid arteries were dissected, gently flushed with PBS to remove residual blood, immediately snap frozen using liquid nitrogen, and kept at −80 °C until use. Segments of thrombi and defined portion of the adjacent injured vessel wall or homogenized heart tissue were ground to tissue powder and lysed with ice-cold RIPA lysis buffer (20 mM Tris-HCl pH 7.5, 150 mM NaCl, 1% Nonidet-P40, 0.5 % Sodium Deoxycholate, 1 mM EDTA, 1% SDS) containing protease inhibitors (Complete Mini, Roche). Lysates were left on ice for 30 min with occasional vortexing and clarified at 16,000 g for 15 min at 4°C to remove cellular debris. Lysates were separated by SDS-PAGE (4-20% Tris-Glycine Gel) and transferred to nitrocellulose membranes with a pore size of 0.2 µm (Schleicher & Schuell). The membranes were probed with a rabbit antibody to mouse TFPI (American Diagnostica), followed by incubation with a secondary, horseradish conjugated antibody to rabbit IgG (Calbiochem). The proteins were visualized by enhanced chemiluminescence according to the manufacturer´s instructions (PerkinElmer Life Sciences).

To assess TFPI degradation in suspensions of blood cells *in vitro*, we activated human platelets (2 x 10^7) and neutrophils (2 x 10^6; isolated with microbeads) for 30 min with

collagen (8 µg ml^{-1}) and thrombin (0.5 U ml^{-1}; 37°C). After centrifugation, we analyzed TFPI degradation in the supernatants recovered from the suspensions of activated blood cells. In other experiments, we used recombinant TFPI (prepared as described above or obtained from a different source (NovoNordisk)). nTFPI and TFPI variants were exposed for 30 min to isolated neutrophil elastase (Calbiochem), cathepsin G (Sigma) or MMP-9 (Sigma). To inhibit cathepsin G and neutrophil elastase, we used alpha-1-antitrypsin, alpha-1-antichymotrypsin (both from Sigma) and CMK (Calbiochem). Western blotting was performed with samples containing equal amounts of proteins using a polyclonal goat antibody to human TFPI (Santa Cruz; 5 µg ml^{-1}) or, where indicated, a monoclonal human TFPI-Kunitz-1 domain-specific antibody (American Diagnostica; 5 µg ml^{-1}). Samples of total supernatant proteins or nTFPI and its variants were then loaded on 12% SDS-PAGE. After electroblotting, the membranes were exposed to TFPI-specific antibodies and, subsequently, to horseradish peroxidase-conjugated secondary antibodies.

For TFPI pull-down experiments, 500 µg recombinant bovine FXa (NEB) was first dialyzed overnight against PBS and covalently coupled to 10 mg Roti®-MagBeads COOH (Roth) using the carbodiimide method according to the manufacturer's recommendation. Subsequently, we lysed isolated mouse platelets in RIPA buffer containing protease inhibitors (Complete Mini, Roche). Lysates were left on ice for 30 min with occasional vortexing and clarified at 16,000 × g for 15 min at 4°C to remove cellular debris. Then we precipitated TFPI from 300 µg of total protein (cellular lysates or plasma) using bovine FXa-coupled Roti®-MagBeads on a rotator overnight at 4°C. The MagBeads beads were washed 5 times with PBS containing Tween 20 (0.05%) and then boiled for 10 min at 70°C in SDS sample buffer. The samples were then subjected to 10% SDS-PAGE and Western blot analysis.

Quantification of released nucleosomes. We activated isolated human platelets (10^9) for 15 min with collagen (type I; 8 µg ml^{-1}) and then incubated them with freshly isolated human neutrophils (ficoll isolation) in the presence of aprotinin (20 µg ml^{-1}) plus PMA (100 nM) for 15 min at 37°C. After centrifugation, we collected the supernatant. In other cases, instead of activation by collagen, we activated platelets for 30 min with LPS (5 µg ml^{-1}, 37°C). They were then incubated for another 15 min in the presence of neutrophils and LPS (37°C). Nucleosomes released from activated neutrophils were determined by Elisa (Cell Death Detection ELISA^{plus}; Roche)[5], which is based on antibodies directed against DNA (single-stranded and double-stranded) and histones (H1, H2A, H2B, H3, and H4).

Procoagulant activity and fibrin generation ex vivo. We determined the procoagulant activities of THP-1 cells (10^5), suspensions of human neutrophils (10^6; isolated with microbeads) incubated for 15 min with either human platelets (10^7) or THP-1 cells, suspensions of mouse neutrophils (5×10^5) incubated for 15 min with mouse platelets (5×10^6), human skin fibroblasts (3×10^3 cells/well), or recombinant tissue factor (Innovin, Dade-Behring; 60 pg/well) using a 2-stage assay in the presence of FVIIa (2 nM; Novo Nordisk) and CaCl$_2$ (25 mM) for 15 min, followed by addition of FX (200 nM; Calbiochem) for 30 min. To degrade their externalized nucleosomes, we pretreated neutrophils with DNase I (10 U ml^{-1}) or clostripain (12 µg ml^{-1}; Worthington). In some cases (where indicated), the procoagulant activity was measured using a coagulation factor concentrate[1]. The amount of FXa generated was assessed using S2222. Fibrin formation in whole blood was estimated by thrombelastography following recalcification of the citrated blood[1]. To inhibit human tissue factor, we used monoclonal and polyclonal antibodies to tissue factor (VIC7 (available at American Diagnostica #4507 in labeled form) and American Diagnostica #4502). For inhibition of mouse tissue factor, TFPI and factor IXa, mouse tissue factor-specific antibody 1H1 (50 µg ml^{-1}), mouse-TFPI- and mouse FIXa-specific antibodies (both from Santa Cruz) were used. Where indicated, we used CTI to prevent activation of the contact pathway of coagulation. In some experiments, the effects of the protease inhibitors CMK (Calbiochem), alpha-1-antitrypsin, alpha-1-antichymotrypsin and TIMP-1 (all from Sigma) on the procoagulant activities were analyzed.

Intravital microscopy. For injury of the carotid artery, we anesthetized WT or *Elane$^{-/-}$;Ctsg$^{-/-}$* mice (12-16 weeks of age) by intraperitoneal injection of a solution of midazolame (5 mg kg^{-1} body weight; Ratiopharm), medetomidine (0.5 mg kg^{-1} body weight; Pfizer), and fentanyl (0.05 mg kg^{-1} body weight; CuraMed Pharma). The common carotid artery was dissected free and endothelial denudation was induced near the carotid bifurcation by a 3-min exposure to FeCl$_3$ or by ligation of the artery for 5 min as described[6]. In brief, for FeCl$_3$-induced injury, the common carotid artery was dissected free and a filter paper (0.5-1.0 mm) saturated with 10% FeCl$_3$ was applied for 3 min to the adventitial surface of the vessel. In the case of ligation injury, the right common carotid artery was dissected free and ligated near the carotid bifurcation for 5 min[6]. We visualized fibrin formation by intravital microscopy[7] using an Alexa488-labeled fibrin IIß chain-specific antibody (Bß 15-42, clone T2G1, Accurate Chemical) infused intravenously (0.3 mg kg^{-1} body weight). Alexa488-labeled isotype-matched irrelevant IgG (mouse IgG2a; Sigma) was used as a negative control. To inhibit

tissue factor-dependent extrinsic pathway and contact pathway-induced activation of coagulation, we injected mouse tissue factor-specific antibody (1H1; 10 µg g^{-1} body weight) and PCK (8 µg g^{-1} of body weight) into the jugular vein before vessel injury. In some experiments, we injected H2A-H2B–DNA–specific antibody or control IgG (each at 4 mg kg^{-1} body weight) into the animals. Where indicated, the adhesion of rhodamine 6G-labeled platelets and acridine orange-tagged leukocytes was monitored simultaneously following vascular injury as described[8]. Fibrin formation was monitored *in vivo* using an Olympus fluorescence microscope equipped with an Orca camera and a 20x (NA 0.95) water-immersion objective. A Siemens workstation with the Cell^R software was used for synchronization of components, data acquisition and image analysis.

Duration of occlusion. We assessed the time to thrombotic occlusion following FeCl$_3$-exposure of the mouse carotid artery as described above. After removal of the filter paper, the time interval was registered until complete arrest of blood flow in the center of the vessel (platelet flow velocity = 0 m s^{-1}). After varying periods of time, flow reappeared in the occluded vessel. The time between the initial occlusion and reestablishment of flow was considered as duration of occlusion.

Thrombus size. We determined the size of the thrombi by measuring the cross-sectional area (visualized with van Gieson stain) of the injured vessel walls by planimetry 30 min after the end of vessel injury.

TFPI incorporation into thrombi. To evaluate incorporation of injected TFPI into thrombi, we injected human TFPI (3 µg/mouse) into WT mice and subsequently injured the carotid artery (FeCl$_3$). We then prepared freeze-dried sections from the excised thrombi. To visualize thrombus-associated platelets, the sections were incubated with mouse CD41-specific antibody (5 µg ml^{-1}, BD Pharmingen) followed by incubation with Alexa594-labeled detection antibody (Invitrogen). Subsequently the sections were treated with Alexa488-labeled human TFPI-specific antibody (Santa Cruz) or respective control antibody (5 µg ml^{-1}, Zymed).

Plasma TFPI. We determined TFPI concentrations in mouse blood plasma by an Elisa assay according to the instructions of the manufacturer (USCN Life Science and Technology). The

concentration of the injected human TFPI in mouse blood was determined by an Elisa specifically detecting human TFPI (Assaypro).

Systemic infection, neutrophil accumulation and CFU counts. We injected GFP-labeled *E. coli* (strain DH12; transfected with GFP-containing plasmid) at an amount of 3.2×10^8 CFU (suspended in 100 µl PBS) into the Vena jugularis of WT and *Elane$^{-/-}$;Ctsg$^{-/-}$ mice*. Where indicated, hirudin (desirudin, 10 mg kg^{-1} body weight, Novartis) or rVIIa (0.5 mg kg^{-1} body weight, Novoseven) were injected into the Vena jugularis 5 min prior to the injection of bacteria. nTFPI and its T87F-L89A mutant were infused (1 µg h^{-1}) during the entire infection period. 6 h after injection of *E. coli*, the livers and spleen were recovered from euthanized animals, directly snap frozen in liquid nitrogen and cut into 10 or 16 µm sections. After fixation with methanol for 10 min at –20°C, the sections were dried, washed four times with PBS and blocked with 2% FBS in PBS containing 0.1% Tween-20 for 1 h at room temperature. After four washing steps, the tissue sections were incubated with CD32-specific antibody (5 µg ml^{-1}) and then with Alexa594-labeled fibrin IIß chain-specific antibody (10 µg ml^{-1}). After the incubations with the antibodies, we washed the sections four times. To visualize bacteria and Kupffer cells, freeze-dried sections were incubated with FITC-labeled GFP- (Rockland Immunochemicals) and Cy3-labeled F4-80-specific antibodies (AbD Serotec). To visualize bacteria, Kupffer cells and neutrophils in paraffin sections, we incubated the sections with rabbit GFP- (Molecular Probes), rat F4-80- (derived from hybridoma cell line at Max-Planck-Institut für Immunbiologie) or rabbit MPO-specific (DAKO) antibodies detected with rat IgG- and rabbit IgG-specific antibodies coupled to Cy2 and Cy5 (Jackson Immuno). The specificity of the staining was verified by analyzing, in parallel, the respective control antibodies labeled with the same fluorophores. Subsequently, 10 consecutive visual fields were analyzed for each animal using a LSM 510 META confocal laser scanning microscope (Carl Zeiss; 40x Plan-Apochromat oil objective and 40x Plan-Neofluar objective). Liver and spleen sinusoids were identified by specific staining with a Alexa546-labeled monoclonal mouse stabilin-2-specific antibody (12 µg ml^{-1}). Data are expressed as fibrin-positive area per luminal area of microcirculatory vessel.

Analysis of multiple stained paraffin sections was carried out on a DMRBE Microscope (Leica Microsystems) equipped with a Nuance Multispectral Imaging system (Cambridge Research & Instrumentation). Fluorescence data were recorded as a set of three image stacks covering the partly overlapping emission ranges of three different long pass filter sets. In total, a spectral range of 500 nm to 720 nm was covered at a step-width of 10

nm. Spectral unmixing was performed utilizing Nuance software version 2.8.0. The single components of the fluorescence signal were extracted from the datasets using defined emission spectra of the fluorophores and the autofluorescence of paraffin embedded tissue as comparison. We obtained a set of component images for each fluorophore, the component representing the autofluorescence being shown in darker neutral grey in order to visualize the tissue surrounding blood vessels.

To measure the number of fibrin-occluded microvessels, we analyzed 10 consecutive visual fields (4×10^4 μm^2 each). We classified microcirculatory vessels in which the lumen was occupied by > 80% with fibrin as occluded vessels. To determine the distribution of bacteria in the hepatic microcirculation, we counted the number of GFP-*E. coli* in the lumen of stabilin-2-positive vessels and in the surrounding tissue of 10 consecutive visual fields (10^5 μm^2 each) for each animal. For every visual field analyzed, we visualized GFP-*E. coli* in the focal plane as well as in planes immediately above and beneath it to assess the localization of the entire pathogen. The observers were unaware of the nature of the samples inspected under the confocal microscope. When 20 identical consecutive visual fields were independently analyzed by two different examiners, the determinations agreed within 4.6-4.9 % (vessel-associated bacteria) and 2.1-6.9% (tissue-associated bacteria).

To quantify the neutrophil accumulation within the vessels, we stained the liver sections with hematoxylin/eosin and counted polymorphonuclear leukocytes in 10 consecutive visual fields for each animal. For determinations of CFUs, 6 h after infection with *E. coli*, blood was collected from the left ventricle and subsequently lung, liver, spleen, and kidney were excised. Then serial dilutions of the homogenized organs and the recovered blood were plated on LB-Ampicillin plates for 16 h and the number of CFU was counted.

Proinflammatory blood parameters. We determined the plasma levels of the chemokine MCP-1 and the cytokine TNFα in systemic blood drawn from the left ventricle of the heart 6 h after injection of *E. coli* using Elisa assays (R&D Systems).

Parameters of liver damage. We determined plasma levels of AST and ALT 6 h after intravenous injection of *E. coli* by photometric measurement of NADH consumption.

Supplementary references

1.   Muller, I. *et al.* Intravascular tissue factor initiates coagulation via circulating microvesicles and platelets. *Faseb J.* **17**, 476-478 (2003).

2.   Boxio, R., Bossenmeyer-Pourié, C., Steinckwich, N., Dournon, C., & Nüsse, O. Mouse bone marrow contains large numbers of functionally competent neutrophils. *J. Leukoc. Biol.* **75**, 604-611 (2004).

3.   Ermert, D. *et al.* Mouse Neutrophil Extracellular Traps in Microbial Infections. *J. Innate Immun.* **1**, 181-193 (2009).

4.   Gawaz, M. *et al.* Incomplete inhibition of platelet aggregation and glycoprotein IIb-IIIa receptor blockade by abciximab: importance of internal pool of glycoprotein IIb-IIIa receptors. *Thromb. Haemost.* **83**, 915-22 (2000).

5.   Holdenrieder, S. *et al.* Nucleosomal DNA fragments in autoimmune diseases. *Ann. N. Y. Acad. Sci.* **1075**, 318-327 (2006).

6.   Massberg, S. *et al.* Platelets secrete stromal cell-derived factor 1alpha and recruit bone marrow-derived progenitor cells to arterial thrombi in vivo. *J. Exp. Med.* **203**, 1221-1233 (2006).

7.   Reinhardt, C. *et al.* Protein disulfide isomerase acts as an injury response signal that enhances fibrin generation via tissue factor activation. *J. Clin. Invest.* **118**, 1110-1122 (2008).

8.   Massberg, S. *et al.* Platelet-endothelial cell interactions during ischemia/reperfusion: the role of P-selectin. *Blood* **92**, 507-515 (1998).